DOI: 10.1002/ejic.201000566

Spectroscopic Characterization and Competitive Inhibition Studies of Azide Binding to a Functional NOR Model

Ying Yang,*[a] Abhishek Dey,[b] and Richard A. Decréau[b]

Keywords: Azides / Azide binding / Nitric oxide reductase model / Competitive inhibition / EPR spectroscopy

Azide binding to a functional nitric oxide reductase (NOR) model has been investigated in its mixed-valence ($LFe^{III}Fe^{II}$ and $LFe^{II}Fe^{III}$) and fully oxidized ($LFe^{III}Fe^{III}$) forms. FTIR and EPR spectroscopic methods indicate that azide binds in a bridging mode between the heme iron and the non-heme iron sites. Terminal azide binding at both heme and non-heme centers is also identified with the reactions of azide and the dinuclear compounds LFe^{III}/Zn^{II} and LZn^{II}/Fe^{III}: the bound azide at the ferric heme center exhibits a vibrational frequency at 2007 cm^{-1} in the FTIR, while the bound azide at the ferric non-heme site shows a band at 2055 cm^{-1}. The reactivity of nitric oxide with the model compounds in the presence of excess azide was investigated. It is demonstrated that azide does not inhibit NO binding to the fully reduced catalyst but binds the Fe_B tightly in both the mixed-valence and the fully oxidized states. These results further support the proposal that a bis-ferrous instead of a mixed-valence state is the active form of NOR.

Introduction

Azide ions can interact with metals of enzyme active sites, particularly cytochrome c oxidase (CcO), as a potent inhibitor.[1] The investigation of azide binding properties at metal centers can provide insight into the structure and function of enzyme active sites. There have been several studies about azide binding at the heme a_3-Cu binuclear site of CcO.[2] Most information was obtained from Fourier transform infrared (FTIR), electron paramagnetic resonance (EPR), and resonance Raman (rR) techniques. However, it is generally a complicated scenario for azide binding to an enzyme due to the presence of other metals and the complex protein structure. Some controversial assignments on the mode of azide binding to bovine cytochrome c oxidase still remain in the literature.[2a–2c] Synthetic biomimetic model complexes provide a more controlled and straightforward platform to study the azide binding at metal centers of a protein active site. One synthetic CcO model has been used to model azide binding with EPR and UV/Vis spectroscopy methods.[3] Recently, we have investigated azide binding to a functional CcO active site model by using UV/Vis, EPR, and FTIR methods.[4] It has been demonstrated that azide can bind to both the resting and the mixed-valence states of the CcO functional model as a bridging ligand between heme and Cu_B.

Nitric oxide reductase (NOR) is a membrane-bound enzyme that catalyzes the $2e^-$ reduction of nitric oxide (NO) to nitrous oxide (N_2O) which is involved in bacterial denitrification. The catalytic subunit of NOR has a very similar structure to that of CcO except that the distal metal Cu_B in CcO is replaced by a non-heme Fe metal in NOR.[5] Unlike CcO, the mechanism of NOR function is still under debate. Both the fully reduced (heme Fe^{II}/Fe_B^{II})[6] and the mixed-valence states (heme Fe^{III}/Fe_B^{II})[7] have been proposed to be the active form of the enzyme. Recently, we have reported the first functional heme/non-heme functional nitric oxide reductase model that can reduce nitric oxide to nitrous oxide forming a bis-ferric product.[8] We demonstrated that the fully reduced bis-ferrous compound instead of the mixed-valence state is active during the NO reduction. In the present work, we investigate azide binding to this heme/non-heme diiron compound. UV/Vis, FTIR, and EPR spectroscopy are used to characterize different modes of azide binding to the diiron site in various oxidation states (LFe^{III}/Fe^{III}, LFe^{III}/Fe^{II}, and LFe^{II}/Fe^{III}). In addition, we studied the competitive binding of nitric oxide and azide at the diiron site. It was found that azide does not inhibit the bis-ferrous form, but does inhibit the mixed-valence form.

Results and Discussion

Synthesis of Model Compounds

Figure 1 shows the representation of the model complexes of ligand L. The monometallic LFe^{III} complex was synthesized by oxidizing the LFe^{II} complex[9] with one equivalent of ferrocenium tetrafluoborate ($FcBF_4$) in THF

[a] Department of Chemistry, University of Toronto, Toronto, ON M5S 3H6, Canada
Fax: +1-416-978-8775
E-mail: yyang@chem.utoronto.ca
[b] Department of Chemistry, Stanford University, Stanford, CA 94305-5080, USA

Supporting information for this article is available on the WWW under http://dx.doi.org/10.1002/ejic.201000566.

as described previously.[4] The bis-ferric compex LFe^{III}/Fe^{III} was generated by oxidation of LFe^{II}/Fe^{II} with two equivalents of ferrocenium tetrafluoroborate. The mixed-valence compound LFe^{III}/Fe^{II} was obtained by oxidation of LFe^{II}/Fe^{II} with one equivalent of $FcBF_4$. The mixed-valence compound $LFe^{II}/Fe^{III}(Br)$ was made by the reaction of LFe^{II} with one equivalent of $FeBr_3$. With the triflate counterion, Fe_B has a higher redox potential than the heme Fe. The soft bromide ligand makes the redox potential of Fe_B more negative, thus it becomes easier to oxidize than the heme Fe. The dinuclear compounds LFe^{III}/Zn^{II} and LZn^{II}/Fe^{III} were synthesized by similar methods from the reactions of LFe^{III} with $Zn(OTf)_2$ and LZn^{II} with $Fe(ClO_4)_3$, respectively.

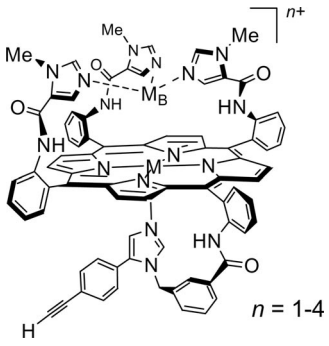

Figure 1. Representation of the model complexes of ligand L: LFe^{II} (M = Fe^{2+}, no M_B); LFe^{III} (M = Fe^{3+}, no M_B); LFe^{III}/Zn^{II} (M = Fe^{3+}, M_B = Zn^{2+}); LZn^{II}/Fe^{III} (M = Zn^{2+}, M_B = Fe^{3+}); LFe^{III}/Fe^{II} (M = Fe^{3+}, M_B = Fe^{2+}); LFe^{III}/Fe^{III} (M = Fe^{3+}, M_B = Fe^{3+}) (M_B has triflate counterions); $LFe^{II}/Fe^{III}(Br)$ (M = Fe^{2+}, M_B = Fe^{3+}) (M_B has Br^- counterions).

Spectroscopic Study of Azide Binding to the Model Compounds

Binding of the azide ion to the monometallic LFe^{III} heme complex in THF causes shifts of both Soret (from 421 nm to 426 nm) and Q (from 544 nm to 550 nm) bands in UV/Vis spectra (Figure 2, solid and dashed lines). For LFe^{III}/Fe^{II}, the Soret band shifts from 421 nm to 425 nm and the Q band shifts from 528 nm to 532 nm upon azide binding (Figure 2, solid and dashed lines with triangle markers). Similar UV/Vis shifts are seen for azide binding to LFe^{III}/Fe^{III}: the Soret band shifts from 419 nm to 426 nm and the Q band shifts from 530 nm to 540 nm (Figure 2, solid and dashed lines with square markers). Binding of azide to $LFe^{II}/Fe^{III}(Br)$ does not cause any band shift, but the intensity of both Soret and Q bands increases (Supporting Information, Figure S1). The addition of azide to LFe^{III}/Zn shifts the Soret band from 423 nm to 426 nm, and the Q band shifts from 535 nm to 540 nm with a shoulder at 562 nm (Supporting Information, Figure S2). For LZn^{II}/Fe^{III}, the Soret band shifts from 430 nm to 432 nm and the Q band shifts from 562 nm to 563 nm upon azide binding (Supporting Information, Figure S3). The above UV/Vis changes indicate that the azide ligates to the iron centers in all cases. Generally, up to 4 equiv. of azide were added to ensure the completion of the binding. Adding more azide did not cause any other changes in the spectra (Figure 2).

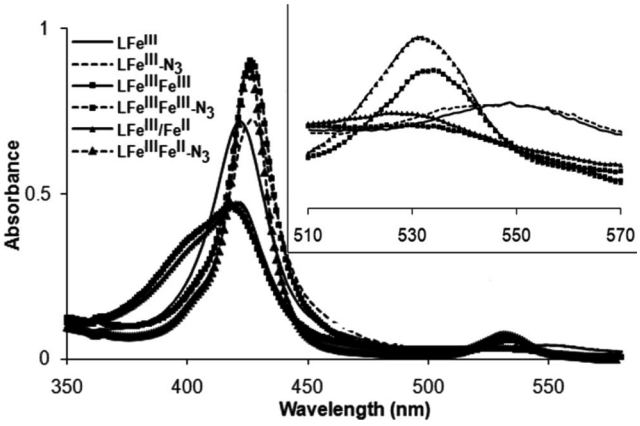

Figure 2. UV/Vis spectra of LFe^{III}, LFe^{III}/Fe^{II}, LFe^{III}/Fe^{III}, $LFe^{II}/Fe^{III}(Br)$, and their azide-bound forms in THF.

FTIR spectroscopy has been proved to be a powerful tool to characterize the properties of azide as it is bound to the metals. The vibrational frequency of bound azides can provide further insight into the structure and function of protein active sites. The FTIR of LFe^{III}-$^{14}N_3$ and LFe^{III}-$^{15}N^{14}N_2$ show similar vibration frequencies to those previously reported.[4] LFe^{III}-$^{14}N_3$ exhibits a peak at 2007 cm^{-1}, while LFe^{III}-$^{15}N^{14}N_2$ shows two bands at 1999 cm^{-1} and 1990 cm^{-1} since azide could bind with either the ^{15}N or ^{14}N atom of the azide (Figure 3, solid and dotted lines). Azide bound to LFe^{III}/Fe^{II} shows a band at 2057 cm^{-1} in FTIR that shifts to 2044 cm^{-1} when $^{15}N^{14}N_2^-$ is used (Figure 3, solid and dotted lines with square markers). This band is 50 cm^{-1} blue shifted relative to that of LFe^{III}-N_3. A similar shift was observed in FTIR spectra for a *bridging* azide between a ferric heme and a distal copper in a CcO model.[4] Binding azide to $LFe^{II}/Fe^{III}(Br)$ exhibits similar bands in FTIR: 2057 cm^{-1} for $LFe^{II}/Fe^{III}(Br)$-$^{14}N_3$ and 2044 cm^{-1} for $LFe^{II}/Fe^{III}(Br)$-$^{15}N^{14}N_2$ (Supporting Information, Figure S4). The azide bands in LFe^{III}/Fe^{III}-N_3 are further shifted to 2065 cm^{-1} and 2051 cm^{-1} when $^{14}N_3^-$ and $^{15}N^{14}N_2^-$ are used, respectively (Figure 3, solid and dotted lines with triangle markers). This further shift of the azide vibrations to higher energy is an indication of its bridging between two oxidized metal sites. This possibility was evaluated using EPR spectroscopy (see below). For all diiron complexes (mixed-valence or fully oxidized), the bridging azide did not show any detectable splitting in FTIR upon replacement of $^{14}N_3^-$ with $^{15}N^{14}N_2^-$, indicating that the strengths of the two internal N=N bonds of azide are very similar to each other.[2a] This is consistent with the azide bridging binding mode with both terminal nitrogen atoms bound to metal centers, leading to the increased effective symmetry of the molecule and therefore less perturbation of the N–N stretch when $^{14}N_3$ is replaced with

$^{15}N^{14}N_2$. The azide bands in mixed-valence complex LFe^{III}/Fe^{II} are wider than those in the fully oxidized complex LFe^{III}/Fe^{III}, which implies a less rigid environment for the azide ligand in the former case.[2d]

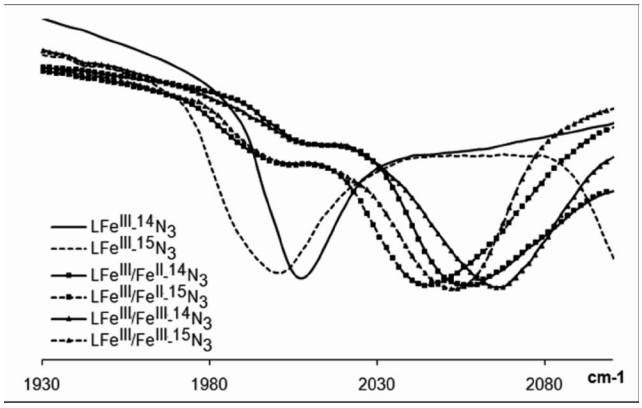

Figure 3. FTIR spectra of the $^{14}N_3$ and $^{15}N^{14}N_2$ derivatives of LFe^{III}, LFe^{III}/Fe^{II}, LFe^{III}/Fe^{III}.

When azide binds to LZn/Fe^{III}, FTIR shows a band at 2055 cm^{-1}. The band shifts to 2043 cm^{-1} when $^{15}N^{14}N_2^-$ is used (Supporting Information, Figure S5). Since binding of azide to the zinc porphyrin is weak,[10] these data show the spectroscopic features of the bound azide at the non-heme distal iron. Binding of azide to LFe^{III}/Zn exhibits mainly the band of ferric heme iron azide in FTIR (Supporting Information, Figure S6), suggesting that a distal Zn^{II} is not a good binding site for azide.

EPR data at 5 K show that the fully oxidized complex $LFe^{III}Fe^{III}$ has a high-spin ferric signal at 1150 G (g = 5.58) and a low-spin ferric signal at 2500–3900 G (g = 2.6, 2.30, 1.98) (Figure 4, solid line). The low-spin signal arises from the heme Fe^{III} (with its strong ligand field)[12] and the high-spin signal arises from the distal Fe_B^{III}. This indicates that the two ferric centers are magnetically uncoupled by exchange implying that there is no bridging ligand between the two paramagnetic centers in the fully oxidized bis-ferric state. When 0.5 equiv. of azide was added, half of the EPR signals were lost (Figure 4, dash-dot line). Binding of 1 equiv. of azide led to the complete disappearance of both ferric EPR signals (Figure 4, dotted line). Thus, N_3^- binds as a bridging ligand between the S = 1/2 heme ferric and S = 5/2 non-heme ferric centers. This enables anti-ferromagnetic coupling between these two sites, leading to an EPR-silent ground state. Since azide is well known for its bridging ability between two metals with M···M distance of 4–6 Å,[13–16] the bridging of the two metals with a single azide implies that, even with the lack of crystallographic data, it is safe to conclude that the distances between the two metals in this model must be ca. 6 Å.[4]

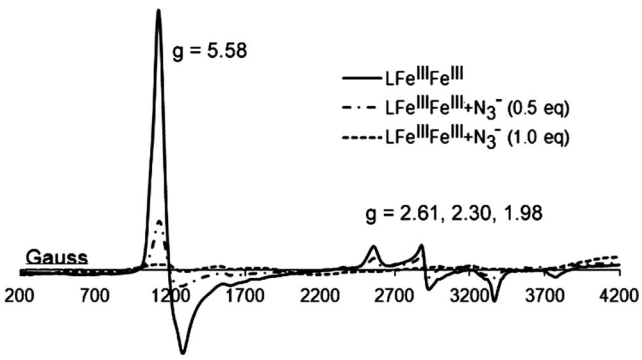

Figure 4. EPR spectra of $LFe^{III}Fe^{III}$ and its azide-bound forms collected at 5 K in frozen THF.

Competitive Binding of Azide and NO at Heme and Non-Heme Iron Sites

We further investigated the competitive binding of nitric oxide to the diiron compound in the presence of excess azide. The reaction of NO with LFe^{II}/Fe^{II} in the presence of excess azide gave a UV/Vis spectrum with bands at 427 nm (Soret), 438 nm, and 550 nm (shoulder) (Figure 5, solid line). Previously we have shown that this reaction, in the absence of azide, generates a LFe^{III}-NO/Fe_B^{III}-OH species.[8] The reaction of NO with azide-bound LFe^{III}/Fe^{III}-N_3 showed the same UV/Vis spectrum (Figure 5, dotted line). They are very similar to the UV/Vis spectrum of the ferric heme nitrosyl LFe^{III}-NO (Figure 5, dash-dot line). The FTIR spectra of the samples from the reactions of NO with $LFe^{II}/Fe^{II}+N_3^-$ and LFe^{III}/Fe^{III}-N_3 exhibit a band at 1925 cm^{-1} (heme ferric nitrosyl) and a band at 2055 cm^{-1} (non-heme ferric azide) (Figure 6). Thus, in both cases the resulting species is a LFe^{III}-NO/Fe_B^{III}-N_3 species. The reaction of NO with the azide-bound mixed-valence compound $LFe^{III}Fe^{II}$-N_3 afforded a UV/Vis spectrum with bands at 424 nm (Soret) and 550 nm (Figure 5, dashed line), which are features of a ferrous heme nitrosyl species.[8] EPR of this sample shows signals featuring both a heme ferrous nitrosyl and a ferric azide (Figure 7, dotted line). This is consistent with the formation of a LFe^{II}-NO/Fe_B^{III}-N_3 species.

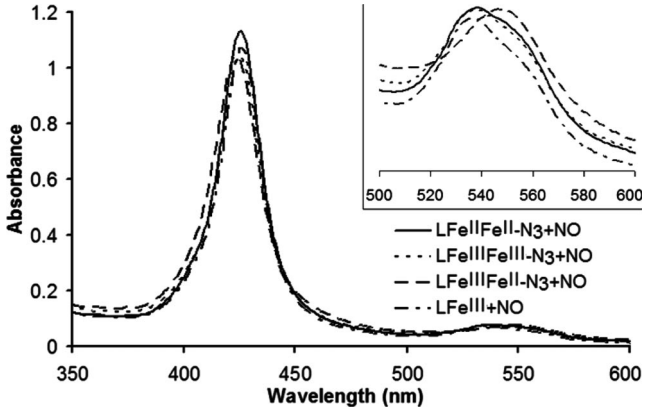

Figure 5. UV/Vis spectra of the products from the reactions of NO with $LFe^{II}/Fe^{II}+N_3^-$, LFe^{III}/Fe^{III}-N_3, LFe^{III}/Fe^{II}-N_3, and LFe^{III} in THF.

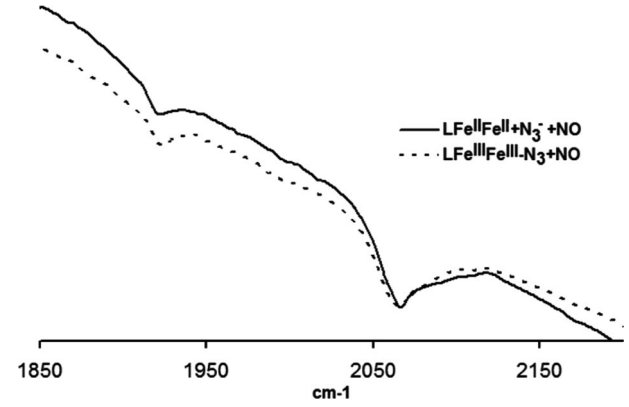

Figure 6. FTIR spectra of the reaction of NO with $LFe^{II}Fe^{II}+N_3^-$ and $LFe^{III}Fe^{III}$-N_3.

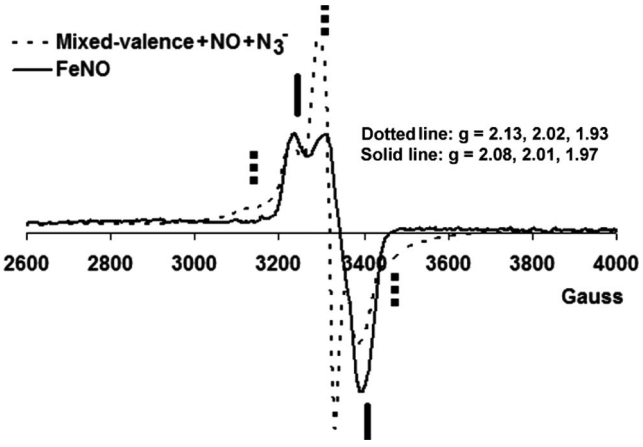

Figure 7. EPR data of LFe^{III}/Fe^{II} + NO + N_3^- (blue line) and an authentic LFe^{II}-NO (red line). The unique signals for the heme ferrous NO are observed in the data and is indicated by red lines. The signals from the distal ferric azide are indicated with blue lines.

Discussion

In this study, it was shown that azide can bind as a bridging ligand between two iron centers of a functional NOR active site model compound, either in its mixed-valence [LFe^{III}/Fe^{II}, LFe^{II}/Fe^{III}(Br)] or fully oxidized states (LFe^{III}/Fe^{III}). This bridging between the two iron metals leads to a blue shift (50–55 cm^{-1}) of azide bands in their FTIR spectra compared to that of LFe^{III}-N_3. This is caused by greater electron density transfer from the N-N π*-type highest occupied molecular orbitals of the bridging azide to the *d* orbitals of two metals coordinated to azide at both sides compared to the azide binding to metal at one side. In the fully oxidized state this bridging interaction resulted in an EPR-silent ground state, indicating anti-ferromagnetic coupling between two iron centers.

We have demonstrated that a bis-ferrous instead of a mixed-valence state is the active form of NOR for the reaction of NO to N_2O. The current investigation of competitive binding of NO and N_3^- at the diiron compound provided further evidence. NO can react quickly with LFe^{II}/Fe^{II} in the presence of excess azide, leading to a LFe^{III}-NO/Fe^{III}-N_3 species. Azide is not a good ligand to the bis-ferrous compound, so the reaction of NO with the bis-ferrous compound is not inhibited by even a large excess of azide and affords the bis-ferric product that can bind azide as a bridging ligand. The bridging azide can be further displaced by NO at the heme ferric site (Scheme 1, A). A controlled experiment with the reaction of NO and the azide-bound bis-ferric compound gave the product with the same spectroscopic features (UV/Vis, FTIR) (Scheme 1, B) as a LFe^{III}-NO/Fe^{III}-N_3 species. The reaction of NO with the azide-bound mixed-valence form afforded the product with a heme ferrous nitrosyl and a non-heme ferric azide (Scheme 1, C). These results demonstrate that NO is a much better ligand than azide for heme iron in its ferrous state. NO, in equimolar amounts, can replace azide bound to the heme iron in its ferric state as well. However, azide has a much higher affinity to a ferric non-heme site than NO. It was reported that azide is not an inhibitor for the reduction of NO to N_2O by NOR.[12] The NO reduction activity of the bis-ferrous compound in the presence of a large excess of azide is consistent with the lack of inhibition by azide and indicates that it is the active form of NOR. On the other hand, the mixed-valence state cannot be the active form of NOR since its reaction with NO is inhibited by azide leading to an LFe^{II}-NO/Fe^{III}-N_3 species which is inconsistent with the inhibition data reported for the enzyme.

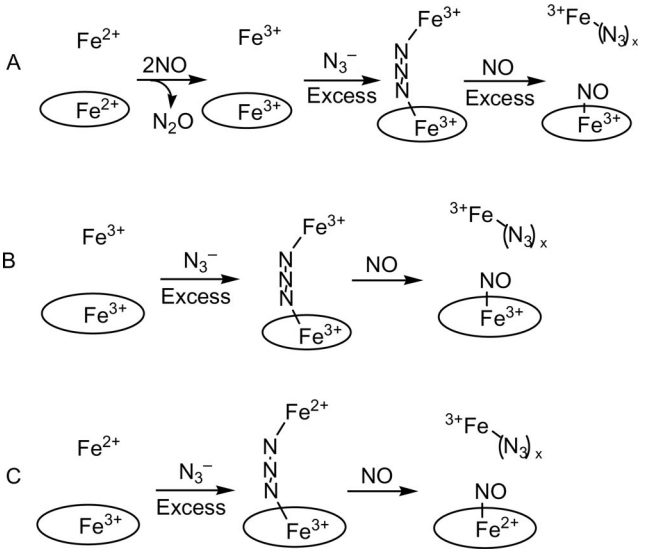

Scheme 1. The reactions of LFe^{II}/Fe^{II}, LFe^{III}/Fe^{III}, and $LFe^{III}Fe^{II}$ with NO in the presence of excess azide.

Conclusions

In conclusion, we have shown that azide can bind as a bridging ligand between heme and non-heme centers in a functional NOR active site model, both in its mixed-valence [LFe^{III}/Fe^{II}, LFe^{II}/Fe^{III}(Br)] and fully oxidized states (LFe^{III}/Fe^{III}). This bridging between the metals results in an anti-ferromagnetically coupled ground state in the fully

oxidized state of the active site. Terminal azide binding at both heme and non-heme centers was obtained from the addition of azide to LFe^{III}, LFe^{III}/Zn, and LZn/Fe^{III} complexes. The bound azide at the ferric heme center exhibits a vibration frequency at 2007 cm^{-1} in FTIR, while the bound azide at the ferric non-heme site shows a band at 2055 cm^{-1} in FTIR. The competitive binding of azide and NO on the diiron center demonstrated that the bis-ferrous instead of the mixed-valence state of the compound is the active form for the reduction of NO to N_2O by NOR.

Experimental Section

General: All reagents were obtained from commercial suppliers and used without further purification unless otherwise indicated. $Fe(OTf)_2(MeCN)_2$ was prepared according to literature procedures.[11] Heme compound LFe^{II} was synthesized as previously reported.[9] All air and moisture-sensitive reactions were carried out under a nitrogen atmosphere in oven-dried glassware. Acetonitrile, tetrahydrofuran, and dichloromethane were purified and dried by passing reagent-grade solvent through a series of two activated alumina columns under a nitrogen atmosphere. These solvents were further deoxygenated by bubbling with nitrogen for 30 min in a nitrogen glove box.

Azide samples for FTIR were made by adding a 1:4 methanol/dichloromethane solution of NaN_3 or $Na^{15}N^{14}N_2$ (95%, IKON isotopes). The amount of N_3^- used varied between 1–2 equiv. between experiments. For EPR, N_3^- was added according to the stoichiometry determined from UV/Vis titrations. The UV/Vis samples were placed in a glass cuvette (3 mL capacity) sealed with a 14/24 septum with sample concentration of about 1×10^{-5} M.

Infrared spectra were obtained with a Mattson Galaxy 4030 FT-IR spectrometer. Solid samples were prepared by dissolving a sample in solution in a glovebox, spotting on a KBr or NaCl palate, and allowing the solvent to evaporate, then covering it by another palate and sealing the sides with Parafilm. The palates containing the sample were sealed in a container and brought to the IR spectrometer for measurement. UV/Vis spectra were recorded with a HP8452 diode array spectrophotometer.

EPR: Bruker EMX spectrometer; X-band; microwave power, 10.0 mW; microwave frequency: 9.38 GHz, modulation frequency: 100.0 kHz; modulation amplitude: 10.0 G, receiver gain: 5.02×103; resolution in X: 1024; T = 77 K or 4.5 K. Sample: (0.5–1.0 mM, 100 μL) in a 4-mm o.d. EPR tube sealed with a septum (Kontes Stopper Sleeve, size 7, 774250-0007) and Parafilm.

Supporting Information (see also the footnote on the first page of this article): Additional UV/Vis and IR spectra for azide binding compounds.

Acknowledgments

This material is based upon work supported by National Institutes of Health (NIH), Grant Number GM-69568-01. We thank Professor James P. Collman for all his guidance and support.

[1] D. Keilin, E. F. Hartree, *Proc. R. Soc. London, Ser. B* **1939**, *127*, 167–191.
[2] a) M. Vamvouka, W. Muller, B. Ludwig, C. Varotsis, *J. Phys. Chem. B* **1999**, *103*, 3030–3034; b) M. Tsubaki, S. Yoshikawa, *Biochemistry* **1993**, *32*, 174–182; c) W. B. Li, G. Palmer, *Biochemistry* **1993**, *32*, 1833–1843; d) S. Yoshikawa, W. Caughey, *J. Biol. Chem.* **1992**, *267*, 9757–9766.
[3] C. Dallacosta, W. A. Alves, A. M. da Costa Ferreira, E. Monzani, L. Casella, *Dalton Trans.* **2007**, 2197–2206.
[4] J. P. Collman, A. Dey, R. A. Decréau, Y. Yang, *Inorg. Chem.* **2008**, *47*, 2916–2918.
[5] a) W. G. Zumft, *Microbiol. Mol. Biol. Rev.* **1997**, *61*, 533–616; b) I. M. Wasser, S. de Vries, P. Moenne-Loccoz, I. Schroder, K. D. Karlin, *Chem. Rev.* **2002**, *102*, 1201–1234.
[6] P. Moenne-Loccoz, S. de Vries, *J. Am. Chem. Soc.* **1998**, *120*, 5147–5152.
[7] a) K. L. C. Gronberg, M. D. Rolda'n, L. Prior, G. Butland, M. R. Cheesman, D. J. Richardson, S. Spiro, A. J. Thomson, N. J. Watmough, *Biochemistry* **1999**, *38*, 13780–13786; b) K. L. C. Gronberg, N. J. Watmough, A. J. Thomson, D. J. Richardson, S. J. Field, *J. Biol. Chem.* **2004**, *279*, 17120–17125.
[8] J. P. Collman, Y. Yang, A. Dey, R. A. Decréau, S. Ghosh, T. Otah, E. I. Solomon, *Proc. Nat. Acad. Sci. USA* **2008**, *105*, 15660–15665.
[9] R. A. Decre'au, J. P. Collman, Y. Yang, Y. Yan, N. K. Devaraj, *J. Org. Chem.* **2007**, *72*, 2794–2802.
[10] Both UV/Vis and FTIR experiments show little changes for the addition of azide to LZn^{II} complex.
[11] K. S. Hagen, *Inorg. Chem.* **2000**, *39*, 5867–5869.
[12] M. Miyata, T. Matsubara, T. Mori, *J. Biochem.* **1969**, *66*, 759–765.
[13] J. Ai, J. A. Broadwater, T. M. Loehr, J. Sanders-Loehr, B. G. Fox, *J. Biol. Inorg. Chem.* **1997**, 37–45.
[14] J. M. Domínguez-Vera, J. Suárez-Varela, I. B. Maimoun, E. Colacio, *Eur. J. Inorg. Chem.* **2005**, 1907–1912.
[15] M. J. Fei, E. Yamashita, N. Inoue, M. Yao, H. Yamaguchi, T. Tsukihara, K. Shinzawa-Itoh, R. Nakashima, S. Yoshikawa, *Acta Crystallogr., Sect. D* **2000**, *56*, 529–535.
[16] M. Moche, J. Shanklin, A. Ghoshal, Y. Lindqvist, *J. Biol. Chem.* **2003**, *278*, 25072–25080.

Received: May 21, 2010
Published Online: September 2, 2010

